The Astrophysical Journal, 680: L65–L68, 2008 June 10

FIRST HIGH SOLAR PHASE ANGLE OBSERVATIONS OF RHEA USING *CASSINI* VIMS: UPPER LIMITS ON WATER VAPOR AND GEOLOGIC ACTIVITY

K. M. Pitman,[1] B. J. Buratti,[1] J. A. Mosher,[1] J. M. Bauer,[1] T. W. Momary,[1] R. H. Brown,[2] P. D. Nicholson,[3] and M. M. Hedman[3]

Received 2008 March 31; accepted 2008 April 29; published 2008 May 21

ABSTRACT

Using radiances acquired with *Cassini*'s Visual and Infrared Mapping Spectrometer (VIMS), we construct high solar phase angle curves for Saturn's second largest moon, Rhea. Ground-based studies of Rhea and Saturnian icy satellites are focussing on low phase angles; to our knowledge, these are the first solar phase curve data for Rhea on phase angles >70°. We compare these data to similar phase curves for Enceladus at near-infrared wavelengths to estimate the amount of water vapor that could possibly be generated and thus set an upper limit on the amount of geologic activity that may be occurring on Rhea. We find that Enceladus's plume manifests itself in the VIMS solar phase curve at a phase angle near 160° and peaks most strongly for $\lambda = 2.017810$ μm. No such peak can be found in the Rhea VIMS phase curve. Absence of a forward scattering peak supports the recent determination that particles in Rhea's surrounding ring are not small. We calculate that the maximum water vapor column density that could be supplied from Rhea ranges from 1.52×10^{14} to 1.91×10^{15} cm^{-2}, 2 orders of magnitude less than what is calculated by *Cassini* UVIS for Enceladus. This implies that for Rhea, the level of active internal (endogenic) processes is exceedingly small, if any.

Subject headings: planets and satellites: individual (Rhea) — solar system: general — techniques: spectroscopic

1. INTRODUCTION

1.1. *Evidence for Activity on Icy Satellites*

The *Cassini-Huygens* mission is currently exploring Saturn and its icy satellites to infer their internal structures and geological histories and activity. Of the Saturnian icy satellites (Mimas, Enceladus, Tethys, Dione, Rhea, Titan, Hyperion, Iapetus, and Phoebe), Titan and Enceladus are known to be geologically active. Evidence for erosion by liquid and winds, tectonism (e.g., mountains and ridges), and, to lesser degrees, cryovolcanism and impact cratering processes, have been noted on Titan (Stofan et al. 2006; Barnes et al. 2007; Radebaugh et al. 2007). The narrow size distribution of H_2O ice particles (0.3–3 μm as measured by the *Cassini* Dust Analyzer [CDA]) in Saturn's tenuous E-ring suggests that, unlike Saturn's F- and G-rings, which are thought to be made of collisional debris, a particular source of water must be responsible for maintaining the E-ring (Jurac et al. 2001). The E-ring, extending from 3 to 8 $R_{\rm Saturn}$ (1 $R_{\rm Saturn}$ = 60,268 km), is believed to be actively and dominantly supplied by H_2O ice particles in geyser-like plumes ejected from "tiger stripe" cracks in the surface of Enceladus (Hansen et al. 2006; Brown et al. 2006; Dougherty et al. 2006; Jones et al. 2006; Porco et al. 2006; Spahn et al. 2006; Spencer et al. 2006; Tokar et al. 2006; Waite et al. 2006). Enceladus's plumes may be feeding Saturn's OH torus as well (Shemansky et al. 1993; Richardson et al. 1998; Johnson et al. 2006). While the first signatures of activity on Enceladus discovered by the *Cassini* Dual-Technique Magnetometer (MAG), CDA, Ion and Neutral Mass Spectrometer, Ultraviolet Imaging Spectrograph (UVIS), and Plasma Spectrometer were concentrated at its south pole, a 2005 November *Cassini* flyby of Enceladus showed multiple sources ejecting water vapor and condensed particles as far as 500 km into space (Porco et al. 2006; Spencer et al. 2006). The *Cassini* Visual and Infrared Mapping Spectrometer (VIMS; Brown et al. 2004), which provides intensity over flux spectra for all of the icy satellites (Filacchione et al. 2007) and the radiance information necessary to construct solar phase curves, has detected alternating bands of crystalline and amorphous water ice on and within the tiger stripes, further suggesting active geologic processes on Enceladus (Brown et al. 2006; Newman et al. 2008). At high phase angles, light emanating from the satellite itself does not contribute; therefore, in a VIMS solar phase curve of Enceladus, plume activity can be seen as a peak beyond ~150°–155°. Forward scattering due to fine grains of water ice contributes to the plume peak; H_2O vapor may also be mixed with the plume material.

There are also indications that other Saturnian icy satellites may be geologically active. The strongest evidence is the detection of plasma transported from Tethys and Dione (Burch et al. 2007). Plasma tori around moons can result from volcanoes (e.g., Io's plasma torus first detected by Kupo et al. [1976] and also seen by *Voyager 1*), and dynamics of volcanic plumes can be affected by plasma arcs (e.g., Gold 1979; Perrat & Dessler 1988). In the report by Burch et al. (2007), double-peaked ("butterfly") pitch-angle distributions of electrons were found in Saturn's inner magnetosphere; when a dipole magnetic field was assumed, higher energy electrons were traced back to Dione (6.26 $R_{\rm Saturn}$) and lower energy electrons were traced back to Tethys (4.88 $R_{\rm Saturn}$). The presence of geologic sources on Tethys and Dione may be investigated more conclusively with MAG in future, close-range *Cassini* flybys; however, such measurements do not preclude searching other data sets for evidence of geologic activity similar to that seen for Enceladus in these and other icy satellites. In this work, we take advantage of newly available *Cassini* VIMS radiance data of Rhea at over twice the range of phase angles previously measured by ground-based or spacecraft observations to search for subtle signs of geologic activity on Rhea, which has "wispy" (faulted) terrain similar to that of Dione.

[1] Jet Propulsion Laboratory, California Institute of Technology, Pasadena, CA; karly.m.pitman@jpl.nasa.gov.
[2] Lunar and Planetary Laboratory, University of Arizona, Tucson, AZ.
[3] Department of Astronomy, Cornell University, Ithaca, NY.

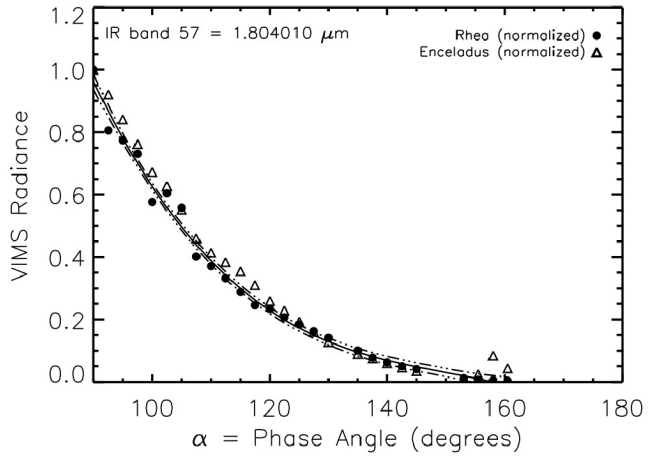

FIG. 1.—*Cassini* VIMS radiance as a function of solar phase angle at quarter to new moon ($\alpha = 90°$–$180°$), for $\lambda = 1.804010$ μm. *Symbols*: Normalized Rhea and Enceladus VIMS radiances (every fifth data point plotted). *Solid line*: Third-order polynomial fit to Rhea data. *Dashed lines*: (polynomial fit to Rhea data) ± 3 σ. Enceladus's plume can be seen as a peak at $\alpha = 159.0°$; the ratio of the Enceladus and Rhea data at that angle is 7.8226187.

1.2. *Investigating Activity on Rhea with Cassini VIMS*

Nine targeted *Cassini* flybys and close serendipitous encounters of Enceladus, Phoebe, Iapetus, Tethys, Dione, Hyperion, and Rhea have already occurred, and many "*Voyager* class" and distant *Cassini* encounters have occurred for these moons and Mimas. The VIMS team has cataloged spectral data for these objects. VIMS is an imaging instrument consisting of two integrated, bore-sighted slit-grating spectrometers with separate reflecting telescopes; the combined spectral range that both VIMS detectors covers is $\lambda \sim 0.34$–5.1 μm. Spatial resolution is as high as 0.25 mrad in the $\lambda \sim 1$–5 μm region and 0.17 mrad in the visible. This unprecedented range in wavelength is coupled with a vastly improved range of solar phase angles as compared to *Voyager* and ground-based observations obtained during the *Cassini* orbital tour. We have searched the VIMS data set for high solar phase angle observations of all of the icy satellites. In the case of Dione, Tethys, and Mimas, VIMS extends to but does not have solar phase angle coverage past $\alpha \sim 155°$; therefore, we cannot directly compare these to Enceladus VIMS data to search for geologic activity at this time. Of the remaining icy satellites, Rhea is particularly well covered by VIMS with a full excursion in solar phase angles from $\alpha \sim 20°$ to $160°$ and some additional data at opposition. Prior to the *Cassini* mission, the highest phase angle at which Rhea had been observed by ground-based or satellite instruments was $\alpha = 68°$ (from *Voyager* narrow-angle camera images; Buratti & Veverka 1984). Rhea is the second largest of Saturn's ~60 moons (*Voyager* imaging radius 764.4 ± 1.1 km [Thomas et al. 2006]; GM $\sim 154.0499 \pm 0.1060$ km^3 s^{-2} [Jacobson et al. 2005]; mean density $\sim 1233 \pm 5$ kg m^{-3}; average geometric albedo ~0.7 [Clark et al. 1986]), with three to six different units of terrain (Moore et al. 1985; Plescia 1985; Wagner et al. 2007 and references therein). Because Rhea is densely cratered and shows little evidence that resurfacing has occurred, most thermal evolution modelers have assumed that medium-sized satellites such as Rhea have undifferentiated interiors (see review by Castillo-Rogez 2006), and Rhea is generally considered to be geologically inactive. The latter view is supported by the *Cassini* UVIS stellar occultation measurement of Rhea, where neutral O was detected in emission but

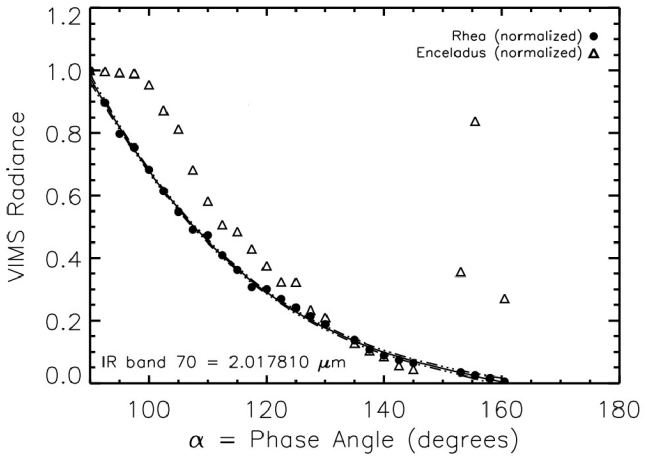

FIG. 2.—Same as Fig. 1, but for $\lambda = 2.017810$ μm. The ratio of Enceladus to Rhea data at the plume peak angle $\alpha = 159.0°$ is 98.094352.

the existence of a plume on Rhea was not observed (Hansen & Hendrix 2007). However, the surface of Rhea shows evidence for extensional tectonism (Pappalardo 2006), suggesting past geologic activity due to tidal forces. Because there has only been one UVIS stellar occultation measurement of Rhea and it covered essentially an equatorial ground track, if a small plume existed on Rhea in an area far removed from the equator, it may have gone undetected (n.b., UVIS did not detect plume activity in the first two Enceladus occultations). If, by constructing a high angle solar phase curve of Rhea, we could set an upper limit on the amount of one of the materials correlated with its plume peak (or lack thereof), we can effectively set a lower limit on the amount of geologic activity on Rhea.

2. OBSERVATIONS AND DATA REDUCTION

By comparing the brightness of Enceladus at its high angle solar phase curve peak to similar data for Rhea, we seek to qualitatively set upper limits on the amount of geologic activity due to tidal forces that may be occurring on Rhea. We first searched for Rhea and Enceladus *Cassini* VIMS observations from $\alpha = 90°$ to $180°$ (quarter to new moon, Figs. 1–3). For Enceladus, we identified equal numbers of points in both the leading and trailing hemispheres at all phase angles. For Rhea, leading and trailing hemispheres are represented for $\alpha \leq 120°$;

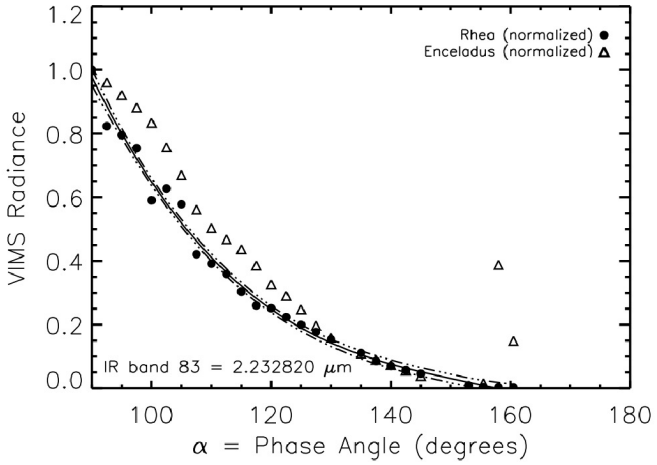

FIG. 3.—Same as Fig. 1, but for $\lambda = 2.232820$ μm. The ratio of Enceladus to Rhea data at the plume peak angle $\alpha = 159.5°$ is 22.578825.

TABLE 1
$P(\lambda) = c_0 + c_1\lambda + c_2\lambda^2 + c_3\lambda^3$ Fit to Rhea VIMS phase curves, Figures 1–3

λ (μm)	c_0	c_1	c_2	c_3	χ^2_{red}
1.804	11.62 ± 0.6171	−0.2237 ± 0.01521	1.462E−03 ± 1.231E−04	−3.236E−06 ± 3.272E−07	1.02092
2.018	9.035 ± 0.3116	−0.1618 ± 7.678E−03	9.888E−04 ± 6.214E−05	−2.064E−06 ± 1.652E−07	0.89740
2.233	11.04 ± 0.6279	−0.2093 ± 0.01547	1.3501E−03 ± 1.252E−04	−2.960E−06 ± 3.329E−07	0.92884

above this range, the Rhea data are from the leading hemisphere. We use data from the VIMS-IR spectrometer only (a detector with a one-dimensional focal plane and two-dimensional instantaneous field of view, spanning $\lambda = 0.8$–5.1 μm at a nominal spectral sampling of 16.6 nm per band), selecting a subset of the 256 total near-infrared wavelength bands: 0.900753, 0.998820, 1.524210, 1.804010, 2.017810, 2.232820, and 3.596100 μm. The motivation for selecting bands below ~3.5 μm is a combination of signal-to-noise ratio detector limits and the fact that ice has low albedo and the solar spectrum is low at $\lambda > 3.5$ μm; the bands selected rest in well-behaved, smooth wavelength intervals with relatively higher H_2O ice reflectance. VIMS returns raw data numbers (DNs) for each spectral channel at each spatial pixel, integrated over an aperture. We flat-fielded and background-subtracted this signal and removed single-pixel, single-spectral channel "spikes" due to cosmic rays and radiation from *Cassini*'s nuclear power generators using the VIMS data calibration pipeline. To convert to radiances, we multiplied the DNs by a radiometric response function for each pixel (Brown et al. 2004, updated by in-flight stellar calibration).

We then removed any remaining instrumental artifacts (McCord et al. 2004), normalized all the VIMS radiances to 1.0 at $\alpha = 90°$, and selected the bands in which the plume of Enceladus peaks in the solar phase curve (occurring at $\alpha \sim 160°$). The Enceladus plume peak shows up most strongly in the $\lambda = 2.017810$ μm data and to lesser degrees in the $\lambda = 2.232820$ and 1.804010 μm phase curves. We fitted these Rhea VIMS radiances with a third-order polynomial (fit parameters given in Table 1). For *Cassini* VIMS radiances of icy satellites in general, a reasonable estimate of error is 5%, given that ground-based observational fluxes have error bars on the order of 5% (4% for good photometry) and that for VIMS data of the Galilean satellites, the largest error for $\lambda = 3.0$–3.8 μm was 5.6% for Callisto (McCord et al. 2004). From the Enceladus reflectance spectra in Newman et al. (2007), a reasonable estimate of error for that moon may be on the order of 3%. Assuming a conservative error in the polynomial fits, we take $+3$ σ from the Rhea radiances at $\alpha \sim 159°$–$160°$ as the upper limit of any plume activity that can be detected by VIMS on Rhea.

3. DISCUSSION

Values are not available for column abundances of H_2O ice originating from Enceladus or Rhea, but column abundances of the lesser component of the plume on Enceladus, H_2O vapor, are available. Therefore, we attempt to estimate an experimental upper limit to the amount of water vapor that could potentially arise from Rhea. We relate the maximum VIMS solar phase curve peak height at $\alpha \sim 160°$ (E) and H_2O vapor column density for Enceladus (n_d) to the radiance value of the $+3$ σ curve fit to the Rhea VIMS data at ~160° (R) to solve for Rhea's maximum possible H_2O vapor column density, X, using

$$\frac{E}{n_d} = \frac{R}{X}. \quad (1)$$

Hansen et al. (2006) give the column density value for H_2O from Enceladus as $n_d = 1.5 \times 10^{16}$ cm^{-2}. This value, derived from *Cassini* UVIS stellar occultation measurements, is for H_2O vapor integrated along the line of sight from the spacecraft to a star through the atmosphere; X is analogously defined for Rhea and is solved for by means of equation (1).

Using equation (1), we calculate that the maximum possible H_2O vapor column density values surrounding Rhea are between 1.52×10^{14} and 1.91×10^{15} cm^{-2}. This estimate does not exceed the total column density budget for neutral H, O, OH, and H_2O modeled for Rhea (Sittler et al. 2008 and references therein). Column abundances of O_3 (a by-product of H_2O dissociation) modeled from *Hubble Space Telescope* observations of Rhea are on the order of $(1–6) \times 10^{16}$ cm^{-2} (Noll et al. 1997). That study suggested that O_2 must be ~500 times more abundant than O_3 around Rhea (i.e., on the order of 10^{18}–10^{19} cm^{-2}); if correct, those numbers imply that our water vapor column density estimates for Rhea are low. Current upper limits for the column densities of [O] and [O_2] around Rhea calculated from UVIS data are 4×10^{13} and 1.5×10^{14} cm^{-2} (Hansen & Hendrix 2007). If we assume that O_2 and H_2O are similar in relative abundance (Ip 2000), our estimates are on par with the abundance values for O_2 that is not morphologically associated with Rhea (Hansen & Hendrix 2007); thus, we posit that there is little, if any, water vapor directly output from Rhea.

Using these estimates and Figures 1–3, we can make several arguments. Although Enceladus is likely the primary contributor of material to the E-ring (Pang et al. 1983; Buratti 1988; Verbiscer et al. 2007), Rhea is in close enough proximity to the outer edge of the E-ring to be a possible, lesser contributor. We have not definitively ruled out Rhea as a contributor (for example, impacts of E-ring particles may kick up particles from Rhea that could be delivered to the E-ring), but we suggest that direct contribution from a plume on Rhea is unlikely, given that the H_2O vapor column densities we calculate for Rhea are 2 orders of magnitude less than what has been derived for Enceladus. Another feature of the Rhea solar phase curve data is relevant to the recently discovered equatorial debris disk composed of grains to decimeter-sized boulders that surrounds Rhea (Jones et al. 2008). The absence of a forward scattering peak in Figures 1–3 suggests that any ice particles resident in this ring cannot be smaller than 1.8–2.2 μm; as small particles tend to be forward scattering, this result may further support that study's determination that particles in Rhea's surrounding ring are not small. For $\lambda = 2.0178$ μm, the Enceladus peak in Figure 2 shows signs of departure beginning at $\alpha = 150°$–$155°$, where VIMS phase angle coverage for other Saturnian icy satellites cuts off. When phase angle coverage be-

yond this point is available, the $\alpha = 150°$–$155°$ range might also be used to constrain activity on Dione, Tethys, and Mimas.

4. CONCLUSIONS

We have constructed the first high solar phase angle curves for Rhea using *Cassini* VIMS radiances, effectively doubling the known solar phase curve for this object. Comparing to plume activity signatures in Enceladus VIMS phase curves at $\alpha \sim 160°$, we estimate that the upper limit to the column abundance of H_2O vapor that could originate from Rhea is 1.52×10^{14}–1.91×10^{15} cm^{-2}. We suggest that, given the comparison to similar values for Enceladus, geologic activity is unlikely to be currently occurring on Rhea. We do not see forward scattering peaks in the VIMS solar radiance data for Rhea, which supports the idea that particles are larger than micron-scale in Rhea's debris disk. When VIMS solar phase angle coverage for Tethys, Dione, and Mimas comparable to the highest solar phase angles for Rhea is available, this method may be used to rate their potential for plume activity as well.

This work was performed at the Jet Propulsion Laboratory, California Institute of Technology, under contract to the National Aeronautics and Space Administration (NASA). The *Cassini-Huygens* mission is a cooperative project of NASA, the European Space Agency, and the Italian Space Agency. Calibrated VIMS data appear courtesy of the VIMS team. K. M. P. is supported by the NASA Postdoctoral Program, administered by Oak Ridge Associated Universities. We thank C. Hansen, A. Hendrix, and J. Castillo-Rogez for helpful conversations and M. McGrath for a helpful review.

REFERENCES

Barnes, J. W., et al. 2007, J. Geophys. Res., 112, E11006, DOI: 10.1029/2007JE002932
Brown, R. H., et al. 2004, Space Sci. Rev., 115, 111
———. 2006, Science, 311, 1425
Buratti, B. J. 1988, Icarus, 75, 113
Buratti, B. J., & Veverka, J. 1984, Icarus, 58, 254
Burch, J. L., et al. 2007, Nature, 447, 833
Castillo-Rogez, J. 2006, J. Geophys. Res., 111, E11005, DOI: 10.1029/2004JE002379
Clark, R. N., Fanale, F. P., & Gaffey, M. J. 1986, in Saturn, ed. T. Gehrels (Tucson: Univ. Arizona Press), 437
Dougherty, M. K., et al. 2006, Science, 311, 1406
Filacchione, G., et al. 2007, Icarus, 186, 259
Gold, T. 1979, Science, 206, 1071
Hansen, C. J., & Hendrix, A. R. 2007, in Workshop on Ices, Oceans, and Fire: Satellites of the Outer Solar System no. 1357 (Houston: LPI), 51
Hansen, C. J., et al. 2006, Science, 311, 1422
Ip, W.-H. 2000, Planet. Space Sci., 48, 775
Jacobson, R. A., et al. 2005, BAAS, 37, 729
Johnson, R. E., et al. 2006, ApJ, 644, L137
Jones, G. H., et al. 2006, Science, 311, 1412
———. 2008, Science, 319, 1380
Jurac, S., Johnson, R. E., & Richardson, J. D. 2001, Icarus, 149, 384
Kupo, I., Mekler, Y., & Eviatar, A. 1976, ApJ, 205, L51
McCord, T. B., et al. 2004, Icarus, 172, 104
Moore, J. M., et al. 1985, J. Geophys. Res. Suppl., 90, C785
Newman, S. F., et al. 2007, ApJ, 670, L143
———. 2008, Icarus, 193, 397
Noll, K. S., et al. 1997, Nature, 388, 45
Pang, K. D., et al. 1983, Lunar Planet. Sci. Conf. 14, 592
Pappalardo, R. T. 2006, Eos Trans. AGU, Fall Meeting Suppl., P32A-02
Perrat, A. L., & Dessler, A. J. 1988, Ap&SS, 144, 451
Plescia, J. B. 1985, NASA-TM 87563, 585
Porco, C. C., et al. 2006, Science, 311, 1393
Radebaugh, J., et al. 2007, Icarus, 192, 77
Richardson, J. D., et al. 1998, J. Geophys. Res., 103, 20245
Shemansky, D. E., et al. 1993, Nature, 363, 329
Sittler, E. C., Jr., et al. 2008, Planet. Space Sci., 56, 3
Spahn, F., et al. 2006, Science, 311, 1416
Spencer, J., et al. 2006, Science, 311, 1401
Stofan, E. R., et al. 2006, Icarus, 185, 443
Thomas, P. C., et al. 2006, Lunar Planet. Sci. 37, 1639
Tokar, R. L., et al. 2006, Science, 311, 1409
Verbiscer, A., et al. 2007, Science, 315, 815
Wagner, R. J., et al. 2007, in Lunar Planet. Sci. Conf. 38, 1958
Waite, J. H., et al. 2006, Science, 311, 1419